TFAP2C is a key regulator of intrauterine trophoblast cell invasion and deep hemochorial placentation

Esteban M. Dominguez[1,*], Ayelen Moreno-Irusta[1], Regan L. Scott[1], Khursheed Iqbal[1,†], and Michael J. Soares[1,2,3,*]

[1]Institute for Reproductive and Developmental Sciences, Department of Pathology & Laboratory Medicine, University of Kansas Medical Center, Kansas City, Kansas 66160, [2]Department of Obstetrics and Gynecology, University of Kansas Medical Center, Kansas City, Kansas 66160, [3]Center for Perinatal Research, Children's Mercy Research Institute, Children's Mercy, Kansas City, MO 64108

[†]Present address: Department of Animal and Food Sciences, Oklahoma State University, Stillwater, Oklahoma

***Correspondence: edominguez@kumc.edu or msoares@kumc.edu**

3901 Rainbow Blvd. Kansas City, KS 66160, Mail Stop 3050.

Phone: 913 588 5960 or 913 588 5961.

Conflict of interests

The authors have declared that no conflict of interest exists.

Abstract

Transcription factor AP-2 gamma (**TFAP2C**) has been identified as a key regulator of the trophoblast cell lineage and hemochorial placentation. The rat possesses deep placentation characterized by extensive intrauterine trophoblast cell invasion, which resembles human placentation. *Tfap2c is* expressed in multiple trophoblast cell lineages, including invasive trophoblast cells situated within the uterine-placental interface of the rat placentation site. Global genome-editing was used to explore the biology of *Tfap2c* in rat placenta development. Homozygous global disruption of *Tfap2c* resulted in prenatal lethality. Heterozygous global disruption of *Tfap2c* was associated with diminished invasive trophoblast cell infiltration into the uterus. The role of TFAP2C in the invasive trophoblast cell lineage was explored using Cre-lox conditional mutagenesis. Invasive trophoblast cell-specific disruption of *Tfap2c* resulted in inhibition of intrauterine trophoblast cell invasion and intrauterine and postnatal growth restriction. The invasive trophoblast cell lineage was not impaired following conditional monoallelic disruption of *Tfap2c*. In summary, TFAP2C contributes to the progression of distinct stages of placental development. TFAP2C is a driver of early events in trophoblast cell development and reappears later in gestation as an essential regulator of the invasive trophoblast cell lineage. A subset of TFAP2C actions on trophoblast cells are dependent on gene dosage.

Introduction

The placenta is a transient organ that ensures viviparity and optimal fetal development (1–3). The human and rat possess a hemochorial placenta (4, 5), which is composed of specialized cellular constituents termed trophoblast cells (6). Among the trophoblast cell lineages contributing to the placentation site are invasive trophoblast cells, which in the human are referred to as extravillous trophoblast cells (7). Human and rat placentation sites are characterized by deep intrauterine trophoblast cell invasion (8–10). Invasive trophoblast cells facilitate the erosion of maternal uterine spiral arteries permitting a direct flow of maternal nutrients to trophoblast cells (8, 11–15). Uterine vasculature remodeling is a critical process ensuring a successful pregnancy outcome (13, 16, 17). There is a paucity of knowledge regarding regulatory mechanisms controlling development of the invasive trophoblast cell lineage and trophoblast cell-guided uterine spiral remodeling.

Members of the transcription factor AP-2 (**TFAP2**) family are key regulators of embryonic and extraembryonic development (18, 19). TFAP2C distinguishes itself as a regulator of the trophoblast cell lineage and hemochorial placentation (20–22). In the mouse, global disruption of the *Tfap2c* locus results in abnormalities within the trophoblast cell lineage and prenatal lethality prior to placentation (23, 24). Although, TFAP2C is an established regulator of the earliest stages of trophoblast cell lineage development (25–28), placental expression profiles and target gene occupancy implicates TFAP2C in the regulation of multiple processes impacting mammalian placentation and placental function (29–40). Included in this broad spectrum of TFAP2C

actions on placentation is its potential involvement in invasive trophoblast cell biology (38–41).

In this report, we present the results of in vivo experimentation directed toward elucidating the physiological role of TFAP2C in the developing hemochorial placenta with a focus on trophoblast cell-guided events within the uterine-placental interface. We show that TFAP2C possesses essential roles during distinct stages of placental development. TFAP2C is an essential regulator of early placental morphogenetic events and reappears in a critical capacity for invasive trophoblast cell lineage development. Finally, elements of TFAP2C actions on placentation are dose dependent.

Results

TFAP2C expression within the placentation site

The rat hemochorial placenta is comprised of multiple lineages of trophoblast cells arranged into distinct compartments, including the labyrinth zone, junctional zone, and uterine-placental interface (42, 43) (Figure 1). The labyrinth zone is the site of maternal-fetal nutrient/waste transfer (44), whereas the junctional zone is composed of endocrine cells targeting the maternal environment and the site where invasive trophoblast cells arise (42, 43, 45). Cell composition of the uterine-placental interface is dynamic, including an increase in the infiltration of invasive trophoblast cells as gestation proceeds (9, 38). Intrauterine invasive trophoblast cells invade into the stroma located between uterine blood vessels (interstitial) and within uterine blood vessels (endovascular). *Tfap2c* transcripts were detected within the uterine-placental interface and increased during pregnancy (Supplemental Figure 1A). In situ hybridization was used to determine the distribution of *Tfap2c* transcripts within the hemochorial placenta. At gestation day (**gd**)

85 9.5, *Tfap2c* was prominently expressed in the ectoplacental cone (Figure 1A). *Tfap2c*
86 transcripts were also localized to the anti-mesometrial uterine deciduum (Figure 1A). As
87 gestation advanced (gd 11.5), *Tfap2c* expression was observed within trophoblast cells of
88 the developing placenta (Figure 1B). On gd 18.5, *Tfap2c* was abundantly expressed within
89 the junctional zone and in invasive trophoblast cells of the uterine-placental interface
90 (Figure 1, C-E). The presence of *Tfap2c* transcripts in the trophoblast cell lineage was
91 supported by its colocalization with keratin 8 (***Krt8***), a pan-trophoblast cell marker (Figure
92 1, A-C). Expression of *Tfap2c* transcripts in invasive trophoblast cells was further
93 demonstrated by co-localization with prolactin family 7, subfamily b, member 1 (*Prl7b1*)
94 transcripts (Figure 1, D and E), an invasive trophoblast cell-specific transcript, and is
95 consistent with single cell RNA-sequencing of the of the uterine-placental interface
96 (Supplemental Figure 1B) (38). TFAP2C protein was distributed in invasive trophoblast
97 cells of the uterine-placental interface and throughout the junctional zone, replicating the
98 distribution of *Tfap2c* transcripts at gd 18.5 (Supplemental Figure 2). Within the invasive
99 trophoblast cell lineage, TFAP2C transcript and protein were localized to both
100 endovascular and interstitial trophoblast cells (Figure 1E**,** Supplemental Figure 3). *Tfap2c*
101 transcripts were localized to most trophoblast cell populations within the junctional zone,
102 including a smaller subset of invasive trophoblast progenitor cell populations (*Prl7b1*
103 positive; Figure 1F).
104
105 **Global deletion of *Tfap2c* leads to prenatal lethality**
106 Next, we investigated the in vivo role of *Tfap2c* in rat placenta development using
107 CRISPR/Cas9 genome editing. DNA-binding and dimerization domains encoded by Exon
108 4 of the *Tfap2c* gene were targeted (Supplemental Figure 4A). A germ line mutant rat was
109 generated possessing a 308-bp deletion within Exon 4 (Supplemental Figure 4B). The

110 deletion resulted in a frameshift and a premature stop codon (Supplemental Figure 4C).
111 Polymerase chain reaction (**PCR**) products corresponding to wild type and mutant alleles
112 were identified by genotyping (828 bp versus 520 bp, respectively, Supplemental Figure
113 4D). Null *Tfap2c* conceptuses (-/-) were obtained by mating heterozygous (+/-) *Tfap2c*
114 females and males. Breeding results collected throughout pregnancy and postnatally,
115 including Mendelian ratios, are presented in Supplemental Table 1. Null *Tfap2c*
116 conceptuses were viable until gd 8.5, which temporally coincides with the onset of
117 placental morphogenesis. This observation agrees with the timing of embryonic demise
118 observed following global *Tfap2c* mouse gene disruption (23, 24). Interestingly, we
119 observed an unexpected reduction in the number of surviving heterozygous pups
120 generated from *Tfap2c*$^{+/-}$ x *Tfap2c*$^{+/-}$, which prompted an investigation of placental
121 development in conceptuses possessing a single *Tfap2c* mutant allele.
122

123 **Decreased *Tfap2c* gene dosage leads to a failure in intrauterine trophoblast cell**
124 **invasion**

125 To explore possible *Tfap2c* gene dosage effects, *Tfap2c*$^{+/+}$ females and *Tfap2c*$^{+/-}$ males
126 were mated, and pregnancies assessed at gd 18.5. *Tfap2c*$^{+/+}$ and *Tfap2c*$^{+/-}$ placentation
127 sites exhibited a similar organizational structure, including a labyrinth zone, junctional
128 zone, and a uterine-placental interface (Figure 2A). We next assessed infiltration of
129 invasive trophoblast cells into the uterine-placental interfaces of *Tfap2c*$^{+/+}$ versus *Tfap2c*$^{+/-}$
130 placentation sites by monitoring the distribution of cytokeratin protein expression (9, 38)
131 (Figure 2B) and *Prl7b1* mRNA (46) (Figure 2C), both representing indices of invasive
132 trophoblast cells. The uterine-placental interface of *Tfap2c*$^{+/-}$ placentation sites were
133 depleted of invasive trophoblast cells (Figure 2, B and C). Both interstitial and
134 endovascular invasive trophoblast cells were diminished in the uterine-placental interface

135 of *Tfap2c*$^{+/-}$ placentation sites. This result was supported by quantification of the depth of
136 invasion of cytokeratin positive cells into the uterine parenchyma (Figure 2D). The
137 depletion of invasive trophoblast cells in the uterine-placental interface of *Tfap2c*$^{+/-}$
138 placentation sites was further supported by diminished expression of several invasive
139 trophoblast cell associated transcripts (*Krt7, Krt8, Krt18, Prl7b1, Prl5a1, Cdkn1c, Cited2,*
140 *Plac1, Peg3, Tfpi;* (38) (Figure 2E). Similar findings were recorded when placentation sites
141 were interrogated from pregnancies generated from *Tfap2c*$^{+/-}$ females mated to *Tfap2c*$^{+/+}$
142 males (Supplemental Figure 5, A-D).
143 However, breeding combinations did differentially affect postnatal heterozygote
144 offspring viability and heterozygote fetal and placental weights. Postnatal heterozygote
145 viability was prominently decreased in female *Tfap2c*$^{+/-}$ x male *Tfap2c*$^{+/-}$ but not in female
146 *Tfap2c*$^{+/+}$ x male *Tfap2c*$^{+/-}$ or female *Tfap2c*$^{+/-}$ x male *Tfap2c*$^{+/+}$ breeding combinations
147 (Supplemental Table 1-3). Genotypic differences in fetal, placenta, junctional zone, and
148 labyrinth zone weights at gd 18.5 were observed among breeding combinations. Mating
149 *Tfap2c*$^{+/+}$ females with *Tfap2c*$^{+/-}$ males was associated with significant decreases in
150 heterozygote placenta, junctional zone, and labyrinth zone weights (Figure 2F), whereas
151 only heterozygote fetal weights were significantly decreased by mating *Tfap2c*$^{+/-}$ females
152 with *Tfap2c*$^{+/+}$ males (Supplemental Figure 5E). Some of these differences might be
153 associated with *Tfap2c* gene dosage effects on the maternal environment.
154

155 **Invasive trophoblast cell conditional *Tfap2c* mutagenesis**

156 The impact of TFAP2C dosage on invasive trophoblast cell development prompted a
157 direct analysis of the importance of TFAP2C on the invasive trophoblast cell lineage. We
158 generated an invasive trophoblast cell-specific *Tfap2c* gene disruption using the Cre/loxP
159 system. CRISPR/Cas9 genome editing was used to insert loxP sites flanking Exon 4 of

160 the *Tfap2c* gene (Figure 3A). *Tfap2c* floxed (***Tfap2c***$^{f/f}$) rats were mated with *Prl7b1-Cre*
161 rats (47). Cre recombinase is specifically targeted to invasive trophoblast cells in *Prl7b1-*
162 *Cre* rats (47). TFAP2C protein was present in lysates of the *Tfap2c*$^{f/f}$ uterine-placental
163 interface but not in lysates of the *Tfap2c*$^{d/d}$ uterine-placental interface (Figure 3B).
164 Immunostaining supported depletion of TFAP2C from the gd 18.5 uterine-placental
165 interface but not from the JZ of *Tfap2c*$^{d/d}$ placentation sites (Figure 3C). Our ability to
166 modulate TFAP2C in the invasive trophoblast cell lineage led us to evaluate a potential
167 role for TFAP2C in regulating the invasive trophoblast cell lineage.
168
169 **TFAP2C-dependent intrauterine trophoblast cell invasion**
170 Intrauterine trophoblast cell invasion was assessed in *Tfap2c*$^{f/f}$ and *Tfap2c*$^{d/d}$
171 placentation sites. At gd 18.5 invasive trophoblast cells were present throughout the
172 *Tfap2c*$^{f/f}$ uterine-placental interface but were not detected in the *Tfap2*$^{d/d}$ uterine-placental
173 interface (Figure 4, A-C). Interstitial and endovascular invasive trophoblast cells were
174 absent from the uterine-placental interface of *Tfap2c*$^{d/d}$ placentation sites. The depletion
175 of invasive trophoblast cells in the uterine-placental interface of *Tfap2c*$^{d/d}$ placentation
176 sites was further supported by diminished expression of several invasive trophoblast cell-
177 associated transcripts (*Krt7, Krt8, Krt18, Prl7b1, Prl5a1, Cdkn1c, Cited2, Plac1, Peg3,*
178 *Tfpi*; Figure 4D). In contrast to the global disruption of *Tfap2c*, migration of invasive
179 trophoblast cells into the uterus was not impaired following conditional monoallelic
180 disruption of *Tfap2c* (Supplemental Figure 6). Single cell RNA-sequencing and single
181 nucleus assay for transposase-accessible chromatin-sequencing datasets (38, 41) reveal
182 a network of genes potentially regulated by TFAP2C in rat invasive trophoblast cells that,
183 include candidate contributors to remodeling extracellular matrix, cytoskeleton
184 restructuring, regulation of cell movement, and transcriptional regulators that target genes

185 encoding other proteins affecting the invasive trophoblast phenotype (Table 1;
186 Supplemental Dataset 1). Thus, TFAP2C has a fundamental role in regulating the invasive
187 trophoblast cell lineage, especially movement of invasive trophoblast cells into the uterus,
188 and a list of downstream effectors are available to investigate mechanisms underlying
189 TFAP2C actions.
190

191 **Invasive trophoblast cells and natural killer (NK) cells exhibit a reciprocal**
192 **distribution within the uterine-placental interface**

193 At midgestation, NK cells are an abundant constituent of the uterine-placental interface
194 (48). As gestation progresses, NK cells become depleted as trophoblast cells invade the
195 uterine-placental interface (48). Interestingly, we observed a retention of NK cells in
196 *Tfap2c*$^{d/d}$ uterine-placental interfaces depleted of invasive trophoblast cells (Figure 5A).
197 This observation was further supported by increased expression of NK cell-associated
198 transcripts (*Prf1, Klrb1c, Klrb1a, Klrb1, Ncr1*; Figure 5B) within *Tfap2c*$^{d/d}$ uterine-placental
199 interfaces. These findings reinforce the observation that fundamental changes occur in
200 the *Tfap2c*$^{d/d}$ uterine-placental interface and imply that invasive trophoblast cells affect
201 cellular dynamics within the uterine-placental interface.
202

203 **Invasive trophoblast cells impact prenatal and postnatal growth**

204 We next investigated whether the presence of invasive trophoblast cells within the
205 uterine-placental interface affected prenatal or postnatal growth. Depletion of invasive
206 trophoblast cells as observed in *Tfap2c*$^{d/d}$ placentation sites was associated with
207 intrauterine placental growth restriction, including both junctional zone and labyrinth zone
208 compartments, and fetal growth restriction at gd 18.5 (Figure 6A). The adverse effects of
209 invasive trophoblast cell depletion on fetal weight extended to postnatal offspring growth.

210 Depletion of invasive trophoblast cells was associated with decreased postnatal body
211 weight (Figure 6B). The results are consistent with invasive trophoblast cells supporting
212 the nutrient demands required for optimal intrauterine growth. Deficits acquired prenatally
213 were sustained during the first three weeks of postnatal life.
214

215 **Discussion**

216 Placentation is a critical adaptation ensuring the success of viviparity (5, 49). Gene
217 manipulated animal models and trophoblast stem cells have provided insights into gene
218 regulatory networks controlling trophoblast cell lineage development and placentation
219 (21). TFAP2C figures prominently in these networks and represents a conserved
220 regulator of placentation (20–22). In the research reported here, we utilized genome-
221 edited rat models to elucidate roles for TFAP2C in placentation. The rat, like the human,
222 is a species exhibiting deep intrauterine trophoblast cell invasion (8–10). TFAP2C is
223 expressed in multiple trophoblast cell lineages of the developing rat placenta, including
224 invasive trophoblast cells residing in the uterine-placental interface. Consistent with
225 earlier reports in the mouse (23, 24), global disruption of *Tfap2c* in the rat led to prenatal
226 lethality (gd 8.5 to 9.5), prior to the initiation of placenta morphogenesis. Interestingly,
227 decreased gene dosage of *Tfap2c* (heterozygous) was compatible with pregnancy but
228 affected placentation, including diminished infiltration of invasive trophoblast cells into
229 the uterine-placental interface. A role for TFAP2C in the regulation of intrauterine
230 trophoblast cell invasion was further supported using cell lineage specific mutagenesis.
231 *Tfap2c* was conditionally disrupted in the invasive trophoblast cell lineage, which led to a
232 uterine-placental interface devoid of invasive trophoblast cells. Impairment of intrauterine
233 trophoblast cell invasion had consequences, including intrauterine and postnatal growth
234 restriction.

235

236 Involvement of TFAP2C in early events dictating trophoblast cell lineage development
237 were reinforced from phenotyping conceptuses possessing a global disruption of the
238 *Tfap2c* locus. TFAP2C is critical to activation of the trophectoderm transcriptome (36,
239 50) and development of trophectoderm (25, 26, 51, 52). Trophectoderm represents the
240 earliest stage of trophoblast cell lineage development (53, 54). The importance of
241 TFAP2C in early trophoblast cell lineage development is further exemplified by its
242 utilization in the direct reprogramming of fibroblasts to the trophoblast cell lineage (27,
243 28).

244

245 TFAP2C actions in the rat placentation site were affected by gene dosage. Monoallelic
246 disruption of *Tfap2c* resulted in the development of a rat uterine-placental interface
247 possessing a diminished number of invasive trophoblast cells. Observing a phenotype in
248 *Tfap2c* global heterozygotes was intriguing but not entirely new for *Tfap2c*.
249 Haploinsufficiency of *Tfap2c* is linked to an increased incidence of peripartum lethality
250 (55). Surviving *Tfap2c* heterozygotes exhibit postnatal growth restriction (24),
251 development of germ cell tumors (56), and hippocampal dysfunction (57). Placentation is
252 also affected by *Tfap2c* haploinsufficiency (55). The labyrinth zone compartment of the
253 mouse placenta is disorganized in *Tfp2c* heterozygotes (55). Interestingly, the invasive
254 trophoblast cell phenotype observed in global heterozygotes reported here was not a
255 feature of conceptuses with a monoallelic disruption of *Tfap2c* restricted to the invasive
256 trophoblast cell lineage. An explanation for this difference is likely connected to the wide-
257 spread involvement of TFAP2C in multiple stages of trophoblast cell differentiation (58).
258 This is supported by TFAP2C expression extending to many more trophoblast cells in
259 the junctional zone than express *Prl7b1*, the gene driving Cre recombinase expression in

our conditional mutagenesis rat model. Global *Tfap2c* haploinsufficiency at a key stage of trophoblast cell lineage development distinct from *Prl7b1*-expressing trophoblast cells must be relevant and responsive to *Tfap2c* gene dosage. Thus, *Tfap2c* gene dosage is utilized in a differentiation stage specific manner to guide trophoblast cell development.

TFAP2C is utilized at different stages of trophoblast cell development. TFAP2C is critical to the derivation of the trophoblast cell lineage and then repurposed for later stages of placentation (58), including the regulation of invasive trophoblast cell development. TFAP2C does not act alone. Context is critical for the actions of TFAP2C. The presence of other transcription factor partners and stoichiometry influence TFAP2C function during trophoblast cell development (21, 59). A short list of potential TFAP2C partners in invasive trophoblast cell development is available (38, 41).

Lastly, we have taken transcript and open chromatin profiles (38, 41) and created a path for elucidating gene involvement in the regulation of invasive trophoblast cell lineage development and its impact on the uterine-placental interface. We provide compelling evidence that TFAP2C is critical in establishing the invasive trophoblast cell lineage. Furthermore, we effectively demonstrate that the presence of invasive trophoblast cells in the uterus has consequences. Deficits in invasive trophoblast cell guided uterine transformation resulted in intrauterine and postnatal growth restriction. Most importantly, tools are in place to establish a gene regulatory network controlling development and function of the invasive trophoblast cell lineage.

In summary, TFAP2C contributes to the progression of distinct stages of rat placental development. TFAP2C is a driver of early events in trophoblast cell development and

285 reappears later in gestation as an essential regulator of the invasive trophoblast cell
286 lineage. A subset of TFAP2C actions on trophoblast cells are dependent on gene
287 dosage.
288
289 **Methods**
290 **Sex as a biological variable**
291 Our study examined male and female animals. Similar findings are reported for both
292 sexes.
293
294 **Animals and tissue collection**
295 Holtzman Sprague–Dawley rats were acquired from Envigo. Animals were maintained
296 in an environmentally controlled facility (14 h light and 10 h dark cycle) with food and
297 water available ad libitum. Timed pregnancies were established using virgin female rats
298 (8 to 10 weeks of age) mated with adult male rats (>3 months of age). Mating was
299 confirmed by the presence of sperm in the vaginal lavage and was considered gd 0.5.
300 Pseudopregnant female rats were generated by mating with vasectomized male rats.
301 Detection of a seminal plug was considered day 0.5 of pseudopregnancy. Pregnant rats
302 were euthanized on specific days of gestation. Some placentation sites were frozen
303 intact in dry-ice cooled heptane and stored at -80 °C for subsequent histological
304 analyses, whereas others were dissected into uterine-placental interface, junctional
305 zone, and labyrinth zone compartments as previously described (38, 60). Dissected
306 placentation site compartments and fetuses were weighed, frozen in liquid nitrogen, and
307 stored at -80°C for subsequent biochemical analyses.
308
309 **Generation of global and conditional *Tfap2c* mutant rat models**

310 A global mutation at the rat *Tfap2c* locus was generated using CRISPR/Cas9 genome
311 editing technology (61). RNA guides targeting Exon 4 of the *Tfap2c* gene (Supplemental
312 Figure 4, Supplemental Table 4) were assembled with *CRISPR* RNA, trans-activating
313 *CRISPR* RNA, and Cas9 nuclease V3 (Integrated DNA Technologies). Conditional
314 *Tfap2c* disruption by the insertion of loxP sites targeted to 5' and 3' introns flanking Exon
315 4 (Figure 3, Supplemental Table 4, and Supplemental Table 5). Electroporation of
316 constructs were performed into one-cell rat embryos using a NEPA21 electroporator
317 (Nepa Gene Co Ltd). Electroporated embryos were transferred to pseudopregnant rats.
318 Offspring were screened for mutations by polymerase chain reaction (**PCR**), and the
319 deletion confirmed by DNA sequencing (GeneWiz). A founder mutant animal was
320 backcrossed with wild type rats to evaluate germline transmission. Genotyping and fetal
321 sex chromosome determination were performed as previously described (47, 61, 62).
322 DNA was extracted from tail-tip biopsies with Red Extract-N-Amp tissue PCR kit (XNAT-
323 1000RXN, Sigma-Aldrich) and used for genotyping. Primers used for genotyping of
324 global and conditional mutations and sex chromosome determinations are provided
325 (Supplemental Table 6). Body weight measurements were performed on offspring
326 generated from specific intercrosses.
327
328 **Reverse transcription-quantitative PCR (RT-qPCR)**
329 Total RNA was isolated from tissues with TRIzol (15596018, Thermo Fisher).
330 Extracted RNA (1 µg) was used to synthesize complementary DNA using a High-
331 Capacity Reverse Transcription kit (4368814, Applied Biosystems) and then diluted 1:10
332 in water. qPCR was performed using PowerSYBR Green PCR Master Mix (4367659,
333 Thermo Fisher) and transcript-specific primer sets (250 nM). Primer sequences are
334 provided (Supplemental Table 7). QuantStudio 5 Real-Time PCR system (Thermo

335 Fisher) cycling conditions were as follows: an initial step (95 °C for 10 min), preceded by
336 40 cycles of two-step PCR (95 °C for 15 s, 60 °C for 1 min), and then a dissociation step
337 (95 °C for 15 s, 60 °C for 1 min), and a sequential increase to (95 °C for 15 s). Relative
338 mRNA expression was calculated using the ΔΔCt method and glyceraldehyde 3-
339 phosphate dehydrogenase was used as a reference RNA.
340
341 **In situ hybridization**
342 In situ hybridization was performed using the RNAscope® Multiplex Fluorescent
343 Reagent kit version 2 (Advanced Cell Diagnostics) according to the manufacturer's
344 instructions. Images were captured on Nikon 90i upright microscopes (Nikon) with
345 Photometrics CoolSNAP-ES monochrome cameras (Roper). Probes were designed to
346 detect *Tfap2c* (860171, NM_201420.2, target region: 696-1733), *Krt8* (87304-C2,
347 NM_199370.1, target region: 134-1472) and *Prl7b1* (860181-C2, NM_153738.1, target
348 region: 28-900).
349
350 **Immunohistochemistry**
351 Frozen rat placentation sites were sectioned at 10 μm, mounted on slides, and fixed in
352 4% paraformaldehyde. Sections were blocked with 10% goat serum (50062Z, Thermo
353 Fisher) and incubated overnight at 4°C with a primary antibody for vimentin (1:300, sc-
354 6260, Santa Cruz Biotechnology), pan-cytokeratin antibody (1:100, F3418, Sigma-
355 Aldrich), perforin (1:300, TP251, Amsbio), or TFAP2C (1:150, 2320, Cell Signaling
356 Technology). Fluorescence-tagged secondary antibodies, Alexa Fluor 488-conjugated
357 goat anti mouse IgG (A11001, Thermo Fisher), and Alexa Fluor 568-conjugated goat
358 anti-rabbit IgG (A11011, Thermo Fisher) were used to visualize immunostaining.
359 Sections were counterstained with 4,6-diamidino-2-phenylindole (DAPI, 1:50,000,

360 D1306, Invitrogen). Slides were mounted in Fluoromount-G (0100-01, SouthernBiotech)
361 and imaged on Nikon 90i upright microscopes with Photometrics CoolSNAP-ES
362 monochrome cameras (Roper). Regions of the uterine-placental interface possessing
363 cytokeratin-positive cells were quantified using ImageJ software, as previously described
364 by our laboratory (63, 64).
365
366 **Western blotting**
367 Tissue lysates were processed using the radioimmunoprecipitation assay lysis
368 buffer (sc-24948A, Santa Cruz Biotechnology) and protein concentrations determined
369 using the DC Protein Assay Kit (5000112, Bio-Rad). Proteins (80 μg/lane) were
370 separated by sodium dodecyl sulfate polyacrylamide gel electrophoresis. Separated
371 proteins were electrophoretically transferred to polyvinylidene difluoride membranes
372 (10600023, GE Healthcare) for 1 h at 25 V on a semi-dry transfer apparatus (Bio-Rad).
373 Membranes were subsequently blocked with 5% milk for 1 h at room temperature,
374 followed by incubation with antibodies to TFAP2C (1:100, sc-12762, Santa Cruz
375 Biotechnology) and GAPDH (1:5,000, AM4300, Invitrogen) in 5% milk overnight at 4°C.
376 After primary antibody incubation, the membranes were washed in Tris-buffered saline
377 with Tween 20 (TBS-T) three times (10 min/wash) at room temperature. The membranes
378 were then incubated with anti-mouse immunoglobulin G conjugated to horseradish
379 peroxidase (HRP; 1:5000, Cell Signaling Technology) in 5% milk for 1 h at room
380 temperature, washed in TBS-T three times (10 min/wash) at room temperature,
381 immersed in Immobilon Crescendo Western HRP Substrate (WBLUR0500, Sigma-
382 Aldrich), and luminescence detected using Chemi Doc MP Imager (Bio-Rad).
383

384 **Identification of TFAP2C and potential TFAP2C gene targets in rat invasive**
385 **trophoblast cells**
386 Uniform manifold approximation and projection (**UMAP**) plots for *Tfap2c* and *Prl7b1*
387 were generated from rat gd 19.5 uterine-placental interface single cell RNA sequencing
388 (accession No. GSE206086, (38)). Gene expression profiles and open chromatin
389 containing TFAP2C DNA binding motifs identified in rat invasive trophoblast cells (38,
390 41) were integrated and ascribed function through manual annotation using the UniProt
391 (https://www.uniprot.org) and National Center for Biotechnology
392 (https://www.ncbi.nlm.nih.gov/) databases.
393
394 **Statistics**
395 Statistical analyses were performed with GraphPad Prism 10.2.3 software. Statistical
396 comparisons were evaluated using Student's *t* test 2-tailed or one-way ANOVA with
397 Tukey's or Dunnett's post hoc tests as appropriate. Statistical significance was
398 determined as $P<0.05$.
399
400 **Study approval**
401 All protocols using rats were approved by the University of Kansas Medical Center
402 Animal Care and Use Committee, Kansas City, Kansas (approved protocol 22-01-220).
403
404 **Data available**
405 All data and materials for this manuscript are included in the Methods and Supporting
406 Data.
407
408 **Author Contributions**

409 E.M.D., K. I., and M.J.S. conceived and designed the research; E.M.D. and A.M-I.,
410 performed experiments; K.I. provided experimental tools for analysis; E.M.D., A.M-I.,
411 R.L.S, and M.J.S. analyzed the data and interpreted results of experiments; E.M.D. and
412 M.J.S. prepared the manuscript. All authors read, contributed to editing, and approved
413 the final version of manuscript.
414

415 **Acknowledgments**

416 We thank Brandi Miller, Stacy Oxley, and Leslie Tracy for administrative assistance.
417 The work was supported by the Lalor Foundation (E.M.D., A.M.-I.), Kansas Idea Network
418 of Biomedical Research Excellence, P20 GM103418 (E.M.D, A.M.-I.), NIH grants:
419 HD115834 (A.M.-I.), HD104495 (R.L.S.), HD104071 (K.I.), HD020676 (M.J.S.),
420 HD105734 (M.J.S.), HD112559 (M.J.S.), and the Sosland Foundation (M.J.S.).
421

422 **References**

423 1. Georgiades P, Ferguson-Smith AC, Burton GJ. Comparative developmental anatomy of the
424 murine and human definitive placentae. *Placenta*. 2002;23(1):3–19.

425 2. Maltepe E, Fisher SJ. Placenta: the forgotten organ. *Annu Rev Cell Dev Biol*. 2015;31:523–552.

426 3. Burton GJ, Fowden AL, Thornburg KL. Placental Origins of Chronic Disease. *Physiol Rev*.
427 2016;96(4):1509–1565.

428 4. Enders AC, Welsh AO. Structural interactions of trophoblast and uterus during hemochorial
429 placenta formation. *J Exp Zool*. 1993;266(6):578–587.

430 5. Roberts RM, Green JA, Schulz LC. The evolution of the placenta. *Reproduction*.
431 2016;152(5):R179-189.

432 6. Hertig AT (Arthur T. *Human trophoblast*. Springfield, Ill. : C. C. Thomas; 1968.

433 7. Vićovac L, Aplin JD. Epithelial-mesenchymal transition during trophoblast differentiation. *Acta*
434 *Anat (Basel)*. 1996;156(3):202–216.

435 8. Pijnenborg R, et al. Review article: trophoblast invasion and the establishment of
436 haemochorial placentation in man and laboratory animals. *Placenta*. 1981;2(1):71–91.

437 9. Ain R, Canham LN, Soares MJ. Gestation stage-dependent intrauterine trophoblast cell
438 invasion in the rat and mouse: novel endocrine phenotype and regulation. *Dev Biol*.
439 2003;260(1):176–190.

440 10. Velicky P, Knöfler M, Pollheimer J. Function and control of human invasive trophoblast
441 subtypes: Intrinsic vs. maternal control. *Cell Adh Migr*. 2016;10(1–2):154–162.

442 11. Kaufmann P, Black S, Huppertz B. Endovascular trophoblast invasion: implications for the
443 pathogenesis of intrauterine growth retardation and preeclampsia. *Biol Reprod*. 2003;69(1):1–7.

444 12. Red-Horse K, et al. Trophoblast differentiation during embryo implantation and formation of
445 the maternal-fetal interface. *J Clin Invest*. 2004;114(6):744–754.

446 13. Pijnenborg R, Vercruysse L, Hanssens M. The uterine spiral arteries in human pregnancy:
447 facts and controversies. *Placenta*. 2006;27(9–10):939–958.

448 14. Harris LK. Review: Trophoblast-vascular cell interactions in early pregnancy: how to remodel
449 a vessel. *Placenta*. 2010;31 Suppl:S93-98.

450 15. Whitley GSJ, Cartwright JE. Cellular and molecular regulation of spiral artery remodelling:
451 lessons from the cardiovascular field. *Placenta*. 2010;31(6):465–474.

452 16. Brosens I, Puttemans P, Benagiano G. Placental bed research: I. The placental bed:
453 from spiral arteries remodeling to the great obstetrical syndromes. *Am J Obstet Gynecol*.
454 2019;221(5):437–456.

455 17. Zhang L, et al. Unraveling the mysteries of spiral artery remodeling. *Placenta*. 2023;141:51–
456 56.

457 18. Hilger-Eversheim K, et al. Regulatory roles of AP-2 transcription factors in vertebrate
458 development, apoptosis and cell-cycle control. *Gene*. 2000;260(1–2):1–12.

459 19. Eckert D, et al. The AP-2 family of transcription factors. *Genome Biol*. 2005;6(13):246.

460 20. Kuckenberg P, Kubaczka C, Schorle H. The role of transcription factor Tcfap2c/TFAP2C in
461 trophectoderm development. *Reprod Biomed Online*. 2012;25(1):12–20.

462 21. Hemberger M, Hanna CW, Dean W. Mechanisms of early placental development in mouse
463 and humans. *Nat Rev Genet*. 2020;21(1):27–43.

464 22. Papuchova H, Latos PA. Transcription factor networks in trophoblast development. *Cell Mol*
465 *Life Sci*. 2022;79(6):337.

466 23. Auman HJ, et al. Transcription factor AP-2gamma is essential in the extra-embryonic lineages
467 for early postimplantation development. *Development*. 2002;129(11):2733–2747.

468 24. Werling U, Schorle H. Transcription factor gene AP-2 gamma essential for early murine
469 development. *Mol Cell Biol*. 2002;22(9):3149–3156.

470 25. Kuckenberg P, et al. The transcription factor TCFAP2C/AP-2gamma cooperates with CDX2 to
471 maintain trophectoderm formation. *Mol Cell Biol*. 2010;30(13):3310–3320.

472 26. Cao Z, et al. Transcription factor AP-2γ induces early Cdx2 expression and represses HIPPO
473 signaling to specify the trophectoderm lineage. *Development*. 2015;142(9):1606–1615.

474 27. Benchetrit H, et al. Extensive Nuclear Reprogramming Underlies Lineage Conversion into
475 Functional Trophoblast Stem-like Cells. *Cell Stem Cell*. 2015;17(5):543–556.

476 28. Kubaczka C, et al. Direct Induction of Trophoblast Stem Cells from Murine Fibroblasts. *Cell*
477 *Stem Cell*. 2015;17(5):557–568.

478 29. Shi D, Kellems RE. Transcription Factor AP-2γ Regulates Murine Adenosine Deaminase Gene
479 Expression during Placental Development*. *Journal of Biological Chemistry*.
480 1998;273(42):27331–27338.

481 30. LiCalsi C, et al. AP-2 family members regulate basal and cAMP-induced expression of human
482 chorionic gonadotropin. *Nucleic Acids Res*. 2000;28(4):1036–1043.

483 31. Sapin V, et al. Differential expression of retinoic acid-inducible (Stra) genes during mouse
484 placentation. *Mech Dev*. 2000;92(2):295–299.

485 32. Ben-Zimra M, et al. Uterine and placental expression of steroidogenic genes during rodent
486 pregnancy. *Molecular and Cellular Endocrinology*. 2002;187(1):223–231.

487 33. Peng L, Payne AH. AP-2 gamma and the homeodomain protein distal-less 3 are required for
488 placental-specific expression of the murine 3 beta-hydroxysteroid dehydrogenase VI gene,
489 Hsd3b6. *J Biol Chem*. 2002;277(10):7945–7954.

490 34. Oztürk A, et al. Proteomic identification of AP2 gamma as a rat placental lactogen II
491 trophoblast cell-specific enhancer binding protein. *Endocrinology*. 2006;147(9):4319–4329.

492 35. Ushizawa K, et al. Global gene expression analysis and regulation of the principal genes
493 expressed in bovine placenta in relation to the transcription factor AP-2 family. *Reprod Biol*
494 *Endocrinol*. 2007;5:17.

495 36. Kidder BL, Palmer S. Examination of transcriptional networks reveals an important role for
496 TCFAP2C, SMARCA4, and EOMES in trophoblast stem cell maintenance. *Genome Res*.
497 2010;20(4):458–472.

498 37. Oikawa M, et al. Generation of Tfap2c-T2A-tdTomato knock-in reporter rats via adeno-
499 associated virus-mediated efficient gene targeting. *Molecular Reproduction and Development*.
500 2022;89(3):129–132.

501 38. Scott RL, et al. Conservation at the uterine–placental interface. *Proceedings of the National*
502 *Academy of Sciences*. 2022;119(41):e2210633119.

503 39. Varberg KM, et al. Extravillous trophoblast cell lineage development is associated with active
504 remodeling of the chromatin landscape. *Nat Commun*. 2023;14(1):4826.

505 40. Kim M, et al. The transcriptional regulatory network modulating human trophoblast stem
506 cells to extravillous trophoblast differentiation. *Nat Commun*. 2024;15(1):1285.

507 41. Vu HTH, et al. Core conserved transcriptional regulatory networks define the invasive
508 trophoblast cell lineage. *Development*. 2023;150(15):dev201826.

509 42. Soares MJ, et al. RAT PLACENTATION: AN EXPERIMENTAL MODEL FOR INVESTIGATING THE
510 HEMOCHORIAL MATERNAL-FETAL INTERFACE. *Placenta*. 2012;33(4):233–243.

511 43. Shukla V, Soares MJ. Modeling Trophoblast Cell-Guided Uterine Spiral Artery Transformation
512 in the Rat. *Int J Mol Sci*. 2022;23(6):2947.

513 44. Knipp GT, Audus KL, Soares MJ. Nutrient transport across the placenta. *Advanced Drug*
514 *Delivery Reviews*. 1999;38(1):41–58.

515 45. Soares MJ, et al. Differentiation of trophoblast endocrine cells. *Placenta*. 1996;17(5–6):277–
516 289.

517 46. Wiemers DO, et al. The mouse prolactin gene family locus. *Endocrinology*. 2003;144(1):313–
518 325.

519 47. Iqbal K, et al. Conditionally mutant animal model for investigating the invasive trophoblast
520 cell lineage. *Development*. 2024;151(2):dev202239.

521 48. Chakraborty D, et al. Natural killer cells direct hemochorial placentation by regulating
522 hypoxia-inducible factor dependent trophoblast lineage decisions. *Proc Natl Acad Sci U S A*.
523 2011;108(39):16295–16300.

524 49. Amoroso EC. The evolution of viviparity. *Proc R Soc Med*. 1968;61(11 Pt 2):1188–1200.

525 50. Li L, et al. Lineage regulators TFAP2C and NR5A2 function as bipotency activators in
526 totipotent embryos. *Nat Struct Mol Biol*. 2024;31(6):950–963.

527 51. Zhu M, et al. Developmental clock and mechanism of de novo polarization of the mouse
528 embryo. *Science*. 2020;370(6522):eabd2703.

529 52. Zhu M, et al. Tead4 and Tfap2c generate bipotency and a bistable switch in totipotent
530 embryos to promote robust lineage diversification. *Nat Struct Mol Biol*. 2024;31(6):964–976.

531 53. Gardner RL, Beddington RS. Multi-lineage "stem" cells in the mammalian embryo. *J Cell Sci*
532 *Suppl*. 1988;10:11–27.

533 54. Rossant J. Stem cells from the Mammalian blastocyst. *Stem Cells*. 2001;19(6):477–482.

534 55. Kaiser S, et al. Reduced Gene Dosage of Tfap2c Impairs Trophoblast Lineage Differentiation
535 and Alters Maternal Blood Spaces in the Mouse Placenta1. *Biology of Reproduction*.
536 2015;93(2):31, 1–13.

537 56. Schemmer J, et al. Transcription factor TFAP2C regulates major programs required for
538 murine fetal germ cell maintenance and haploinsufficiency predisposes to teratomas in male
539 mice. *PLoS One*. 2013;8(8):e71113.

540 57. Loureiro-Campos E, et al. Constitutive deficiency of the neurogenic hippocampal modulator
541 AP2γ promotes anxiety-like behavior and cumulative memory deficits in mice from juvenile to
542 adult periods. *Elife*. 2021;10:e70685.

543 58. Sharma N, et al. Tpbpa-Cre-mediated deletion of TFAP2C leads to deregulation of Cdkn1a,
544 Akt1 and the ERK pathway, causing placental growth arrest. *Development*. 2016;143(5):787–
545 798.

546 59. Latos PA, et al. Elf5-centered transcription factor hub controls trophoblast stem cell self-
547 renewal and differentiation through stoichiometry-sensitive shifts in target gene networks.
548 *Genes Dev*. 2015;29(23):2435–2448.

549 60. Ain R, et al. Phenotypic analysis of the rat placenta. *Methods Mol Med*. 2006;121:295–313.

550 61. Iqbal K, et al. Catechol-O-methyltransferase and Pregnancy Outcome: an Appraisal in Rat.
551 *Reprod Sci*. 2021;28(2):462–469.

552 62. Dhakal P, Soares MJ. Single Step PCR-Based Genetic Sex Determination for Rat Tissues and
553 Cells. *Biotechniques*. 2017;62(5):232–233.

554 63. Rosario GX, Konno T, Soares MJ. Maternal hypoxia activates endovascular trophoblast cell
555 invasion. *Dev Biol*. 2008;314(2):362–375.

556 64. Nteeba J, et al. Poorly controlled diabetes mellitus alters placental structure, efficiency, and
557 plasticity. *BMJ Open Diabetes Res Care*. 2020;8(1):e001243.

558

559

Figures

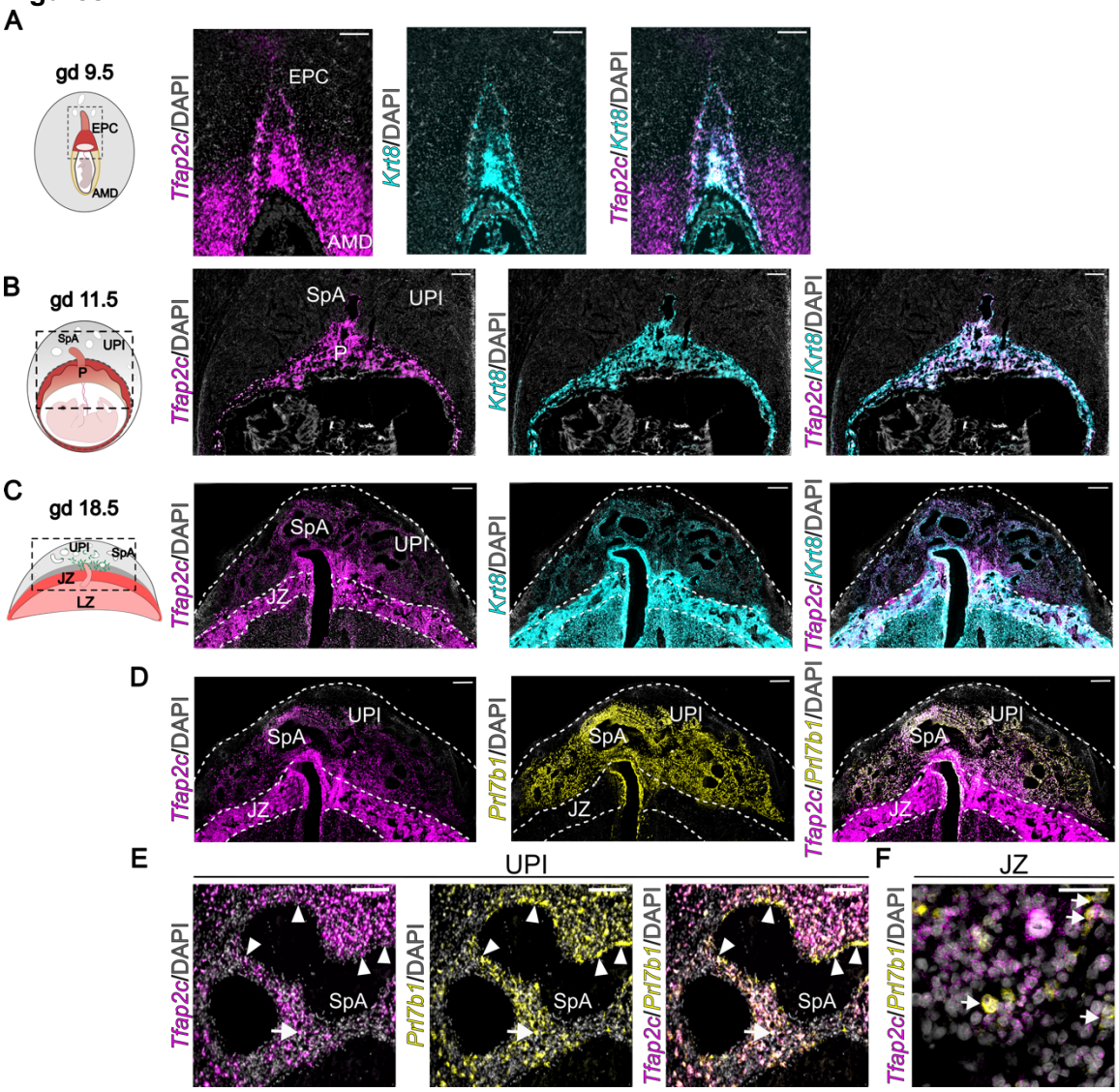

Figure 1. *Tfap2c* transcript distribution during placenta development. (**A-C**) *Tfap2c* transcripts (magenta) were localized to the ectoplacental cone at gestation day (gd) 9.5 (**A**) and placentation sites at 11.5 (**B**), and 18.5 (**C**). *Tfap2c* transcripts were co-localized with *Krt8* transcripts (cyan). Schematic diagrams representing gd 9.5, 11.5, and 18.5 placentation sites are initially presented for each panel. (**D**) Co-localization of *Tfap2c* (magenta) and *Prl7b1* (yellow) transcripts within the gd 18.5 placentation site. *Prl7b1* is specifically expressed in the invasive trophoblast cell lineage. Scale bar: 500 μm. (**E**) High magnification images showing *Tfap2c* and *Prl7b1* transcript localization in endovascular (arrowhead) and interstitial (arrow) invasive trophoblast cells within the uterine-placental interface. Scale bar: 100 μm. (**F**) Co-localization of *Tfap2c* and *Prl7b1* transcripts (arrows) within the junctional zone of the gd 15.5 placenta. Scale bar: 50 μm. Co-localization is shown as whilte. Abbreviations: EPC, ectoplacental cone; AMD, anti-mesometrial decidua; SpA, spiral artery; UPI, uterine-placental interface; P, placenta; JZ, junctional zone; LZ, labyrinth zone.

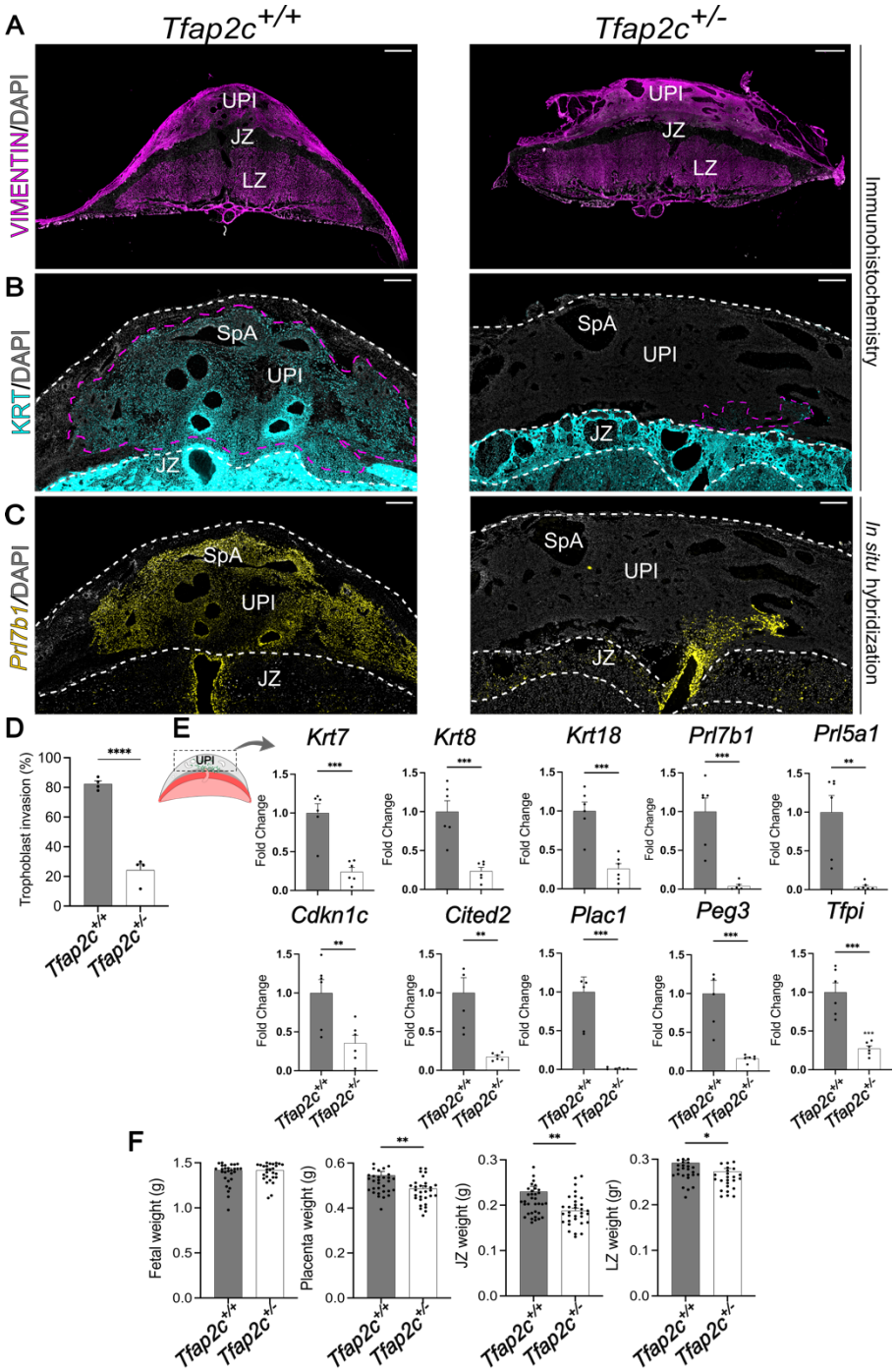

576

577 **Figure 2. *Tfap2c* gene dosage effects on placental development.** Placentation sites
578 were generated from *Tfap2c*$^{+/-}$ male and *Tfap2c*$^{+/+}$ female breeding. (**A**) Identification of
579 placentation site compartments *Tfap2c*$^{+/+}$ and *Tfap2c*$^{+/-}$ using vimentin immunostaining
580 (magenta). (**B**) Immunohistochemical localization of cytokeratin protein in gestation day
581 (gd) 18.5 *Tfap2c*$^{+/+}$ and *Tfap2c*$^{+/-}$ placentation sites (cyan). (**C**) Distribution of *Prl7b1*
582 transcripts in gd 18.5 *Tfap2c*$^{+/+}$ and *Tfap2c*$^{+/-}$ placentation sites (yellow). (**D**)
583 Quantification of trophoblast cell invasion area (magenta dotted line) determined by

584 cytokeratin immunostaining within the uterine-placental interface. Data are expressed as
585 mean ± standard error of the mean (SEM). Each data point represents different uterine-
586 placental interface tissues (n=4) obtained from four pregnancies. (**E**) RT-qPCR of
587 invasive trophoblast cell-specific transcripts in gd 18.5 *Tfap2c*$^{+/+}$ and *Tfap2c*$^{+/-}$ uterine-
588 placental interface tissues. Data are expressed as mean ± SEM. Each data point
589 represents a biological replicate obtained from six different pregnancies (n=6). (**F**) Fetal,
590 placenta, junctional zone and labyrinth zone weights for gd 18.5 *Tfap2c*$^{+/+}$ and *Tfap2c*$^{+/-}$
591 conceptuses. Data are expressed as mean ± SEM. Each data point represents a
592 biological replicate obtained from six different pregnancies (*Tfap2*+$^{+/+}$, n=38; *Tfap2c* $^{+/-}$,
593 n=32). Unpaired *t*-test: * $p<0.05$, ** $p<0.01$, *** $p<0.001$, **** $p<0.0001$. Abbreviations:
594 UPI, uterine-placental interface; JZ, junctional zone; LZ, labyrinth zone; SpA, spiral
595 artery. Scale bars: 500 μm.

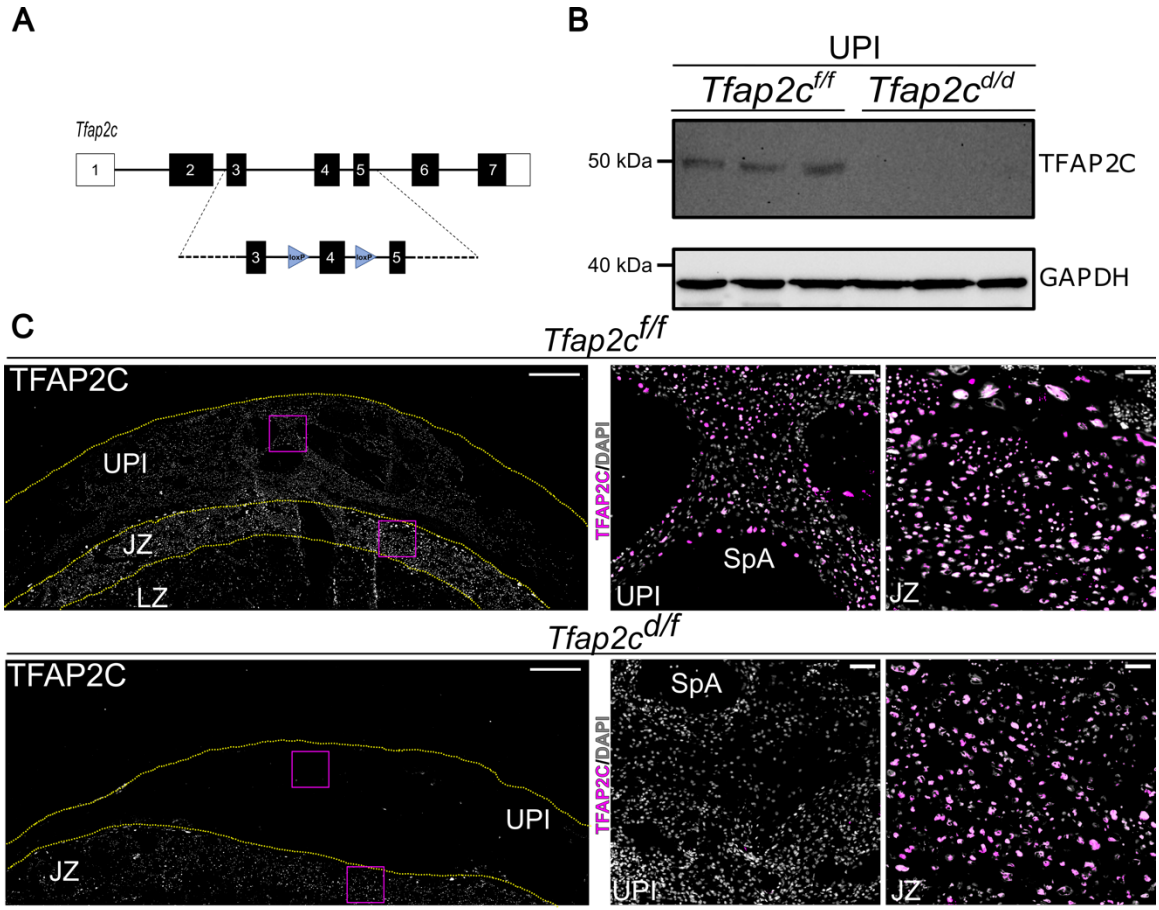

Figure 3. Generation of an invasive trophoblast cell-specific *Tfap2c* deletion. (**A**) Schematic of *loxP* sites inserted into introns flanking Exon 4 of the *Tfap2c* gene. (**B**) TFAP2C western blot of the uterine-placental interface of *Tfap2c*$^{f/f}$ and *Tfap2c*$^{d/d}$ gd 18.5 placentation sites. (**C**) TFAP2C immunostaining of *Tfap2c*$^{f/f}$ and *Tfap2c*$^{d/d}$ gd 18.5 placentation sites (left panels: TFAP2C immunostaining, white; right panels: TFAP2C immunostaining, magenta, DAPI, white). Scale bar: 500 μm. Inserts to the right show higher magnification images of uterine-placental interface tissues (top) and junctional zone tissue (bottom) for each placentation site. Scale bar: 100 μm. Abbreviations: UPI, uterine-placental interface; JZ, junctional zone; LZ, labyrinth zone; SpA, spiral artery.

607

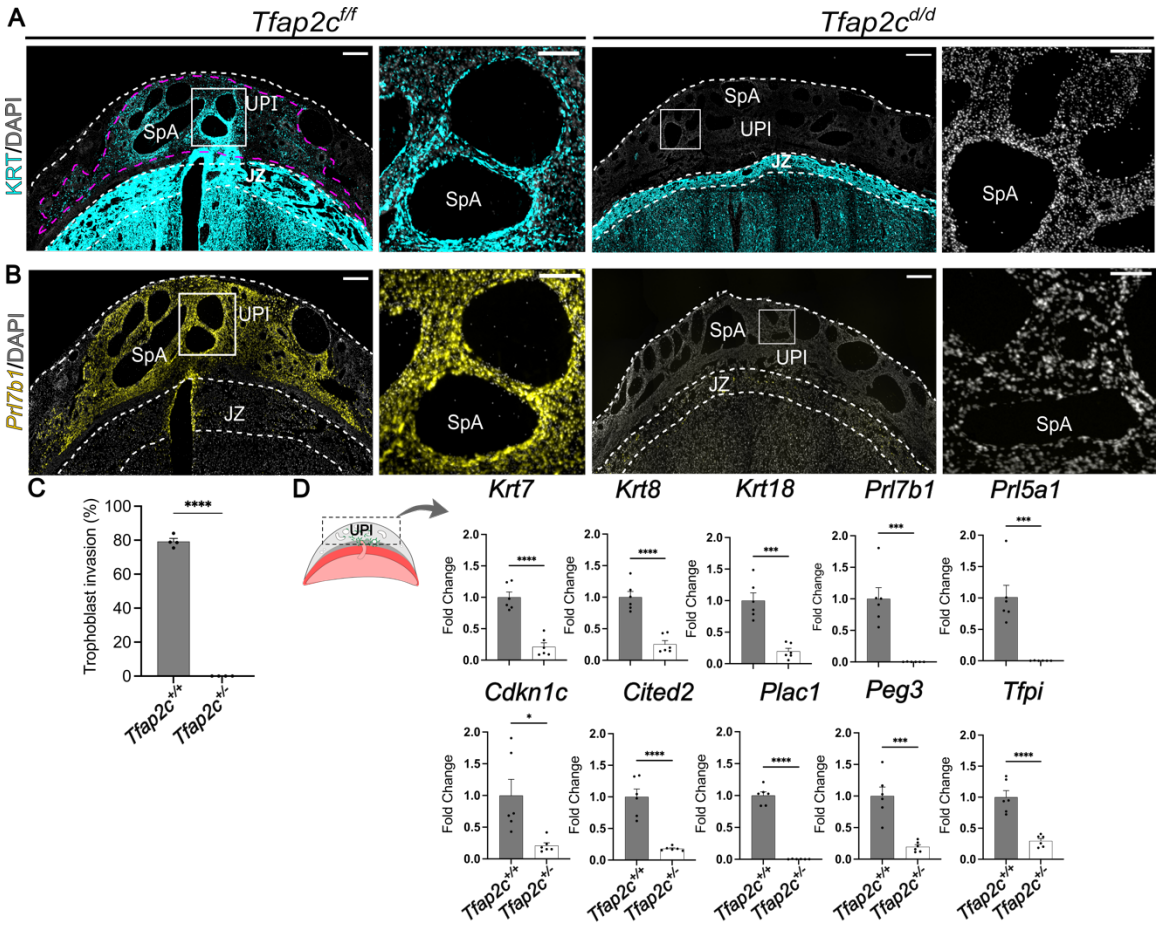

608 **Figure 4. Characterization of invasive trophoblast cell-specific *Tfap2c* deletion.** (**A**)
609 Immunohistochemical localization of cytokeratin (magenta) in gd 18.5 *Tfap2c*$^{f/f}$ and
610 *Tfap2c*$^{d/d}$ placentation sites. (**B**) Distribution of *Prl7b1* transcripts (yellow) in gd 18.5
611 *Tfap2c*$^{f/f}$ and *Tfap2c*$^{d/d}$ placentation sites. Scale bar: 500 μm. Inserts to the right show
612 higher magnification images of the boxed areas within the uterine-placental interface
613 tissues for each placentation site. Scale bar: 100 μm. (**C**) Quantification of trophoblast
614 cell invasion area (green dotted line) determined by cytokeratin immunostaining within
615 the uterine-placental interface. Data are expressed as mean ± standard error of the
616 mean (SEM). Each data point represents different uterine-placental interface tissues
617 obtained from four pregnancies (n=4). (**D**) RT-qPCR of invasive trophoblast cell-specific
618 transcripts in gd 18.5 *Tfap2c*$^{f/f}$ and *Tfap2c*$^{d/d}$ uterine-placental interface tissues. The left
619 panel corresponds to a schematic of the regions of the placentation site used for
620 analysis. Data are expressed as mean ± SEM. Each data point represents a biological
621 replicate from six different pregnancies (n=6). Unpaired *t*-test: *p< 0.05, ***p<0.001,
622 ****p<0.0001.). Abbreviations: UPI, uterine-placental interface; JZ, junctional zone; LZ,
623 labyrinth zone; SpA, spiral artery.
624

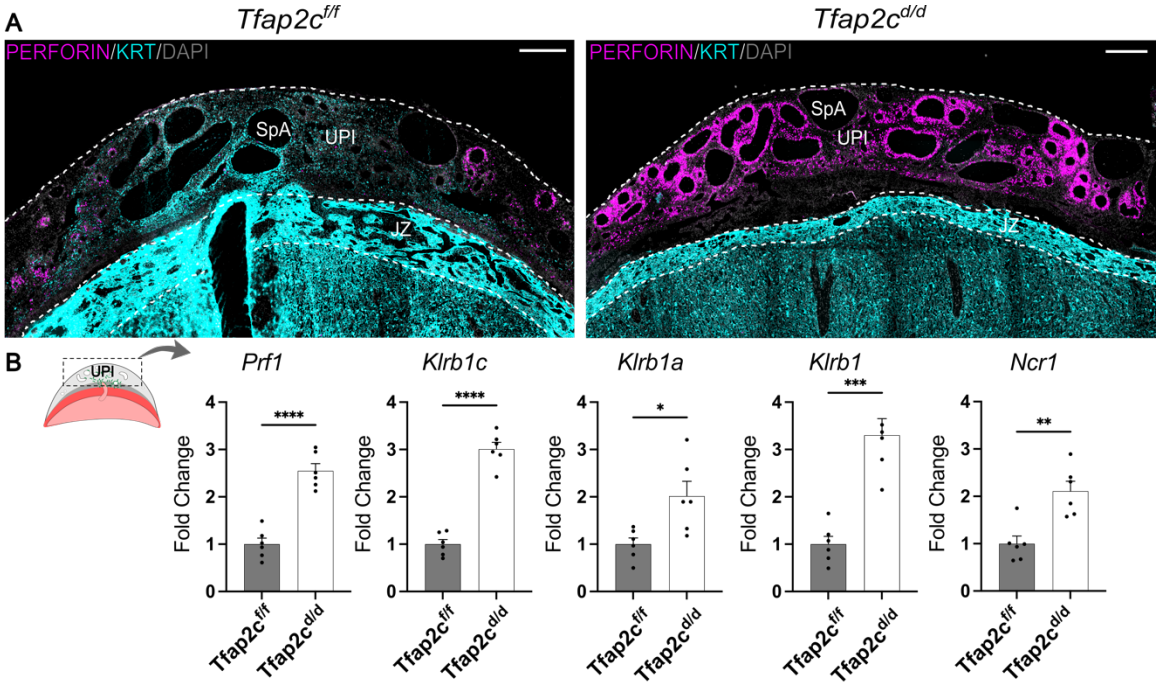

Figure 5. *Tfap2c* conditional deletion in trophoblast invasive cells results in the retention of uterine natural killer (NK) cells within the uterine-placental interface. (**A**) Immunohistochemical localization of cytokeratin (cyan) and perforin (magenta) in gd 18.5 *Tfap2c*$^{f/f}$ and *Tfap2c*$^{d/d}$ placentation sites. (**B**) RT-qPCR of NK cell-specific transcripts in gd 18.5 *Tfap2c*$^{f/f}$ and *Tfap2c*$^{d/d}$ uterine-placental interface tissues. The left panel corresponds to a schematic of the regions of the placentation site used for analysis. Data are expressed as mean ± standard error of the mean. Each data point represents a biological replicate from six different pregnancies (n=6). Unpaired *t*-test: *p< 0.05, **p<0.01, ***p<0.001, ****p<0.0001. Abbreviations: UPI, uterine-placental interface; JZ, junctional zone; LZ, labyrinth zone; SpA, spiral artery. Scale bar: 500 μm. Specimens used in this figure are the same used in Figure 4A.

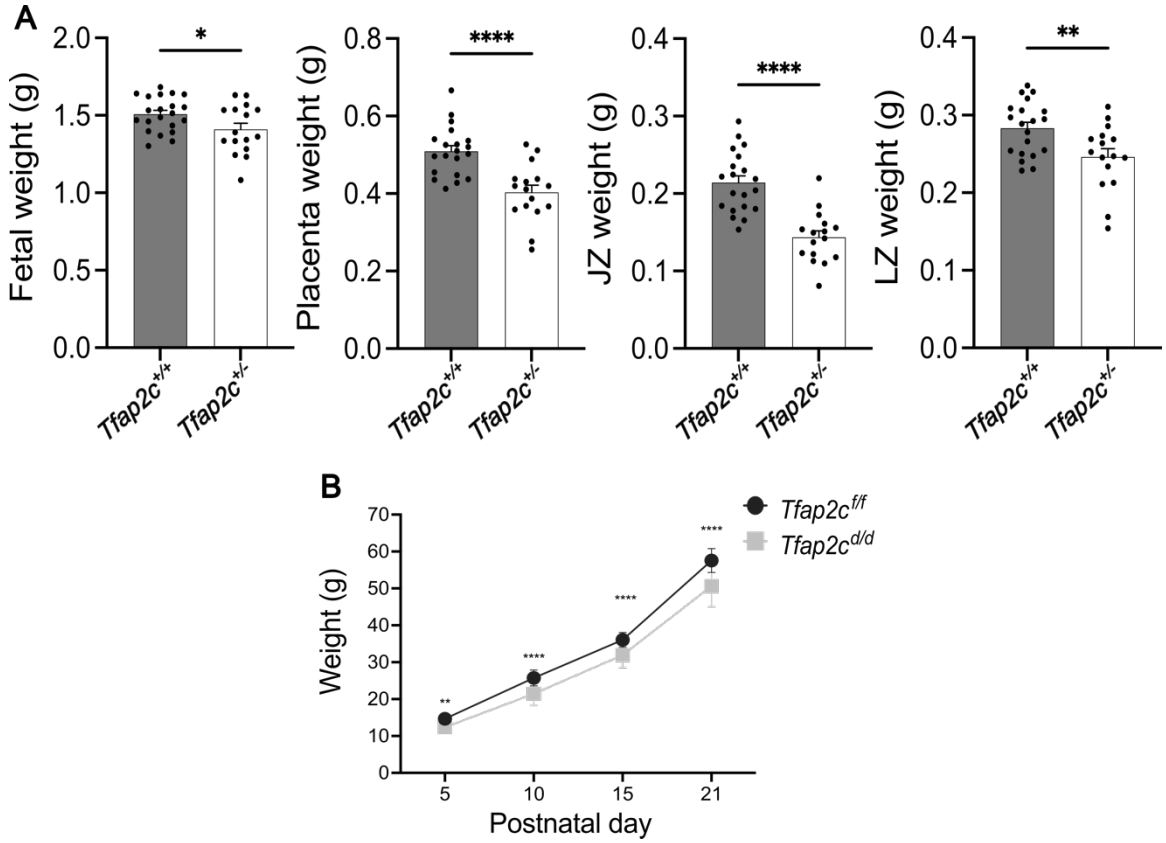

Figure 6. Impact of an invasive trophoblast cell-specific *Tfap2c* deletion on prenatal and postnatal development. (**A**) Fetal, placenta, junctional zone, and labyrinth zone weights from gd 18.5 *Tfap2c*$^{f/f}$ and *Tfap2c*$^{d/d}$ gd 18.5 conceptuses. Data are expressed as mean ± standard error of the mean (SEM). Each data point represents a biological replicate from six pregnancies (*Tfap2c*$^{f/f}$, n=20; *Tfap2c* $^{d/d}$, n= 16). Unpaired *t*-test: *p< 0.05, **p<0.01, ***p<0.001, ****p<0.0001. (**B**) Postnatal body weight for *Tfap2c*$^{f/f}$ and *Tfap2c*$^{d/d}$ pups. Data are expressed as mean ± SEM from six pregnancies (*Tfap2c*$^{f/f}$, n=24; *Tfap2c* $^{d/d}$, n= 29). One-Way ANOVA and Tukey's Test: **p<0.01, ****p<0.0001. Abbreviations: JZ, junctional zone; LZ, labyrinth zone.

652 **Table 1. Subset of genes expressed in invasive trophoblast cells possessing**
653 **TFAP2C DNA binding motifs**

Extracellular matrix organization	Cell movement - migration	Cytoskeletal organization	Transcriptional regulation
Adamts3, Adgrg6	Amotl2, Arhagp8,	Ankrd17, Apbb1ip	Barx2, Bend5
Col4a1	Cald1, Dab2ip	Cald1, Cfl2	Cdx2, Cited2
Fbln1	Efnb1, Fbln1	Daam1	Ets2, Hdac4
Galnt6	Mta3, Ncam1	Dsp	Hic2, Jdp2
Lama4	Nuak1, Parva	Klhl2	Ncor2, Nr2f6
Lamb1	Pcdh12, Plet1	Krt7	Nrip1, Peg3
Nid1	Sema6d, Septin4	Krt8	Pparg, Tfap2c
Tp53i11	Svil, Tbc1d9	Svil	Zfp706

654
655

656 **Supplemental information**

657 Figures S1 to S6 and Table S1 to S7.

658 Dataset S1. Excel file.